

INFRARED CIRRUS AND DISCRETE SOURCES IN THE OUTER GALAXY

MICHEL FICH

Physics Department, University of Waterloo, Waterloo, Ontario, CA N2L 3G1

SUSAN TEREBEY

*IPAC, California Institute of Technology and Jet Propulsion Laboratory,
M/S 100-22, Pasadena, CA 91125*

INTRODUCTION

Studies of Galactic infrared cirrus have been based on (1) observations of individual high latitude clouds (e.g. Boulanger, Baud, and van Albada 1985), (2) analysis of large scale emission at high latitudes in the Scaler Neighborhood (e.g. Boulanger and Perault 1988), and (3) complete linear decomposition of the global emission from IRAS and other observations over the entire Galaxy (e.g. Sodrowski et al 1989, Bloemen, Deul, and Thaddeus 1990).

Here we present preliminary results using a different approach: a detailed analysis of all of the sources of infrared emission, as detected by IRAS, in two large fields in the outer Galaxy. We study both the extended diffuse component, which is primarily associated with H₂ gas, and the discrete, 60 micron bright infrared sources, which are generally star forming complexes at distances of several kpc. We identify and carefully measure from the IRAS images a complete flux-limited sample of discrete sources, and make detailed comparisons with the measured values in other IRAS data products. The discrete sources are compact but extended at the IRAS resolution with the result that significantly more flux is measured on the images than is quoted in the Point Source Catalog.

We study the diffuse (infrared cirrus) component by masking out regions containing discrete sources of molecular clouds and derive the infrared colors of the cirrus emission. In practice the masking procedure has little effect on the results because the emission from discrete sources is found to be several orders of magnitude less than the emission from the cirrus component at all IRAS wavelengths.

DATA ANALYSIS

Because confusion problems are much lower in the outer Galaxy we focused on two regions of the galactic plane bounded by (1) $l = 120^\circ$ to $l = 130^\circ$ and (2) $l = 213^\circ$ to $l = 223^\circ$ and by $b = -10^\circ$ to $b = +10^\circ$. These regions are devoid of large optically known H II regions but are otherwise not special. To find all the star forming regions we examined the 60 micron images from the IRAS Sky Flux Plates (now replaced by the IRAS Sky Survey Atlas (ISSA)) and coadded

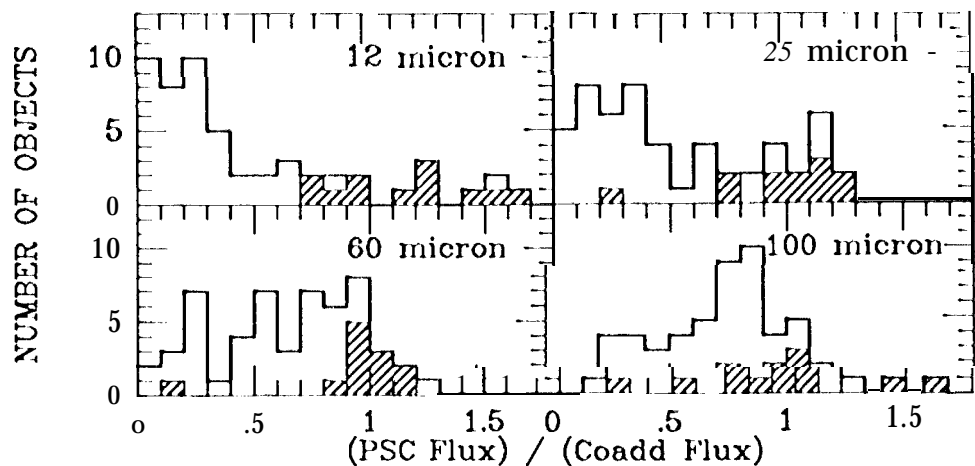


FIGURE 1 Comparison of PSC and image fluxes.

images resulting in a source list that is complete for objects with 60 micron flux densities greater than 25 Jy and radii less than 10 arcminutes. The structure of the star formation regions was complex and so for detailed analysis we used the 2 degree coadded images produced at IPAC that provided the full resolution of the IRAS survey (IRISCO).

The flux above the local background was determined, where in most cases the background value used was the median flux density found in the pixels along the boundary of each object. The background determination dominates the uncertainties in the flux densities, which are estimated to be 44%, 20%, 21 %, and 32% for 12, 25, 60, and 100" microns.

Comparing our discrete source list with the PSC we find that nearly all sources have a corresponding entry in the PSC. The PSC positions are generally more accurate than we can easily determine from the images but the PSC fluxes are often significantly smaller. This is not surprising since the data on which the PSC is based has been processed with a point source filter which effectively suppresses extended structure.

All of the complex sources and most of the simple sources have very similar Flux Density Distributions (FDD's). We expect the complex sources to be mixtures of interstellar clouds and star forming regions and we have defined a distribution of FDD, called Class A that contains all of these sources. Other sources are collectively called Class B and probably are primarily stars.

In Figure 1 the flux density ratios for all four wavebands are shown as histograms with the Class B sources marked with diagonal lines. It is clear that the PSC is underestimating the total flux for the Class A sources and this effect is most dramatic at 12 and 25 microns where the IRAS spatial resolution is greatest (approximately 1 arcmin) and that there is the least effect at 100 microns (approximately 4 arcmin) resolution. The median flux ratios for the Class B sources are all approximately 1, which would be expected if the sources

in this class are unresolved. For the Small Scale Structure Catalog (SSSC) we find matches with fewer of our sources, suggesting that the SSSC is incomplete. The SSSC has poorer positions than the PSC but better correspondence of the fluxes.

After removing all of the discrete sources from our two fields (by masking out these sources on mosaics of ISSA images of the entire (two) fields) we compared the fluxes in each band for each individual field. We first compared the total flux in this diffuse emission to the total in discrete components. For each field and each band Table 1 lists the total flux for all PSC entries in the field, the total flux from the PSC for all of our selected discrete sources, the total flux as measured in the coadd (FRISCO) images for all our selected sources, and the total diffuse emission in the mosaic (ISSA) images within the fields. A zero level correction has been applied to the ISSA values. However the ISSA images in the $l = 218^\circ$ field, which have a relatively low ecliptic latitude of 30° degrees, are clearly contaminated by residual zodiacal emission at the shorter wavelengths. The affected values in Table 1 are shown in parenthesis to indicate they are not reliable measures of the diffuse galactic emission.

Table I shows: (1) the diffuse emission completely dominates the emission in all bands; (2) the flux measured from the images for discrete sources is a factor of 2 to 4 greater than the PSC flux for all of our objects; and (3) at 12 microns our sample only represents a small fraction of all of the flux detected in the PSC.

TABLE 1 Flux Density Totals (in Jy).

$l = 125^\circ$ field	12 microns	25 microns	60 microns	100 microns
All PSC entries	4268.6	3190.3	72(39.1)	14735.2
discrete sources (PSC)	1269.0	1870.5	6181.0	10066.5
discrete sources (Coadd)	2256.5	3679.7	21199.7	38920.1
diffuse emission (ISSA)	8.8×10^3	8×10^4	4×10^5	1.9×10^6
$l = 218^\circ$ field	12 microns	25 microns	60 microns	100 microns
All PSC entries	2549.4	2156.6	4873.0	8952.5
discrete sources (PSC)	229.0	1063.6	4002.8	5596.4
discrete sources (Coadd)	785.2	1700.7	9264.5	17881.9
diffuse emission (ISSA)	(1.1×10^3)	(2.6×10^4)	2.2×10^5	1.6×10^6

For each field we plot the diffuse emission in one band versus another in order to measure the infrared colors (flux ratios) of the diffuse component. To minimize contamination by the star-forming regions we have masked out all the discrete sources. For example, Figure 11 for the $l = 125^\circ$ field shows a linear correlation of the 60 micron versus the 100 micron flux. The derived 60/100 micron ratio confirms our earlier result using the IRAS All Sky Images (Terebey and Fich 1986). However the new ISSA images, which are considerably more sensitive, allow us to extend the analysis to 12 and 25 microns as well.

The derived colors for the $l = 125^\circ$ field are listed in Table 11. The values

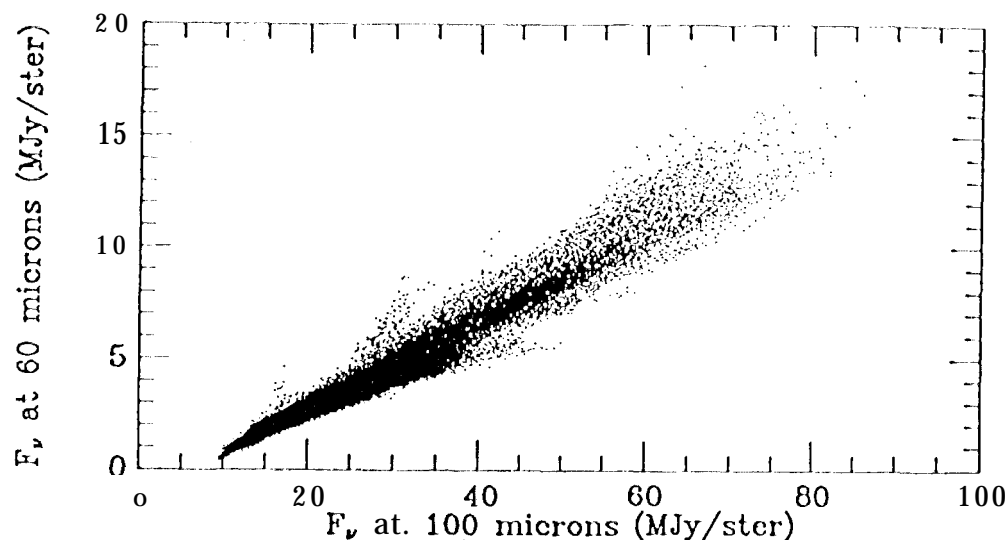


FIGURE 11 The diffuse emission in the $l = 125^\circ$ field.

shown are the mean of the minimum and maximum slopes of data in the plots and the uncertainties given reflect the maximum range in the fits. The colors are consistent with those derived by Boulanger and Perault (1988) for high latitude cirrus. This suggests that the diffuse galactic emission in the outer Galaxy and the local high latitude cirrus are produced under similar physical conditions.

TABLE II Mean Flux Density Ratios (Colors) of Diffuse Galactic Emission.

$60\ \mu m / 100\ \mu m$	$25\ \mu m / 100\ \mu m$	$12\ \mu m / 100\ \mu m$	$25\ \mu m / 60\ \mu m$	$12\ \mu m / 25\ \mu m$
0.2034 ± 0.004	0.0434 ± 0.012	0.046 ± 0.004	0.216 ± 0.071	1.10 ± 0.10

A much more detailed description of the IRAS analysis is in the final stages of manuscript preparation at this time. A comparison with observations at other wavelengths is currently underway.

ACKNOWLEDGMENTS

This work was carried out in part at the Jet Propulsion Laboratory, California Institute of Technology, under a contract with the National Aeronautics and Space Administration.

REFERENCES

- Bloemen, J. B. G. M., Deul, F. R., and Thaddeus, P. 1990, *A&A*, 233, 437
- Boulanger, F., Baud, B., and van Albada, G. D. 1985, *A&A*, 144, L9
- Boulanger, F. and Perault, M. 1988, *ApJ*, 330, 964
- Sodrowski, J. J., Dwek, E., Hauser, M. G., and Kerr, F. "J. 1989, *ApJ*, 1989, 762
- Terebey, S. and Fich, M. 1986, *ApJ*, 309, 1,73